



ARL-TR-7472 • SEP 2015



Synthesis, Transfer, and Characterization of Nanoscale 2-Dimensional Materials

by Travis M Tumlin, Lily Giri, and Mark H Griep

Approved for public release; distribution is unlimited.

NOTICES

Disclaimers

The findings in this report are not to be construed as an official Department of the Army position unless so designated by other authorized documents.

Citation of manufacturer's or trade names does not constitute an official endorsement or approval of the use thereof.

Destroy this report when it is no longer needed. Do not return it to the originator.



Synthesis, Transfer, and Characterization of Nanoscale 2-Dimensional Materials

by Travis M Tumlin and Lily Giri

Oak Ridge Institute for Science and Education

Oak Ridge, TN

Mark H Griep

Weapons and Materials Research Directorate, ARL

REPORT DOCUMENTATION PAGE				<i>Form Approved OMB No. 0704-0188</i>
Public reporting burden for this collection of information is estimated to average 1 hour per response, including the time for reviewing instructions, searching existing data sources, gathering and maintaining the data needed, and completing and reviewing the collection information. Send comments regarding this burden estimate or any other aspect of this collection of information, including suggestions for reducing the burden, to Department of Defense, Washington Headquarters Services, Directorate for Information Operations and Reports (0704-0188), 1215 Jefferson Davis Highway, Suite 1204, Arlington, VA 22202-4302. Respondents should be aware that notwithstanding any other provision of law, no person shall be subject to any penalty for failing to comply with a collection of information if it does not display a currently valid OMB control number.				
PLEASE DO NOT RETURN YOUR FORM TO THE ABOVE ADDRESS.				
1. REPORT DATE (DD-MM-YYYY) September 2015	2. REPORT TYPE Final		3. DATES COVERED (From - To) August 2014–August 2015	
4. TITLE AND SUBTITLE Synthesis, Transfer, and Characterization of Nanoscale 2-Dimensional Materials			5a. CONTRACT NUMBER	
			5b. GRANT NUMBER	
			5c. PROGRAM ELEMENT NUMBER	
6. AUTHOR(S) Travis M Tumlin, Lily Giri, and Mark H Griep			5d. PROJECT NUMBER	
			5e. TASK NUMBER	
			5f. WORK UNIT NUMBER	
7. PERFORMING ORGANIZATION NAME(S) AND ADDRESS(ES) US Army Research Laboratory ATTN: RDRL-WMM-A Aberdeen Proving Ground, MD 21005-21005-5069			8. PERFORMING ORGANIZATION REPORT NUMBER ARL-TR-7472	
9. SPONSORING/MONITORING AGENCY NAME(S) AND ADDRESS(ES)			10. SPONSOR/MONITOR'S ACRONYM(S)	
			11. SPONSOR/MONITOR'S REPORT NUMBER(S)	
12. DISTRIBUTION/AVAILABILITY STATEMENT Approved for public release; distribution is unlimited.				
13. SUPPLEMENTARY NOTES				
14. ABSTRACT In the present work, we have demonstrated the synthesis of graphene, hexagonal boron nitride, and bismuth telluride using chemical and physical vapor deposition techniques. Making these materials cost-effective and scalable is paramount for their integration in a variety of applications. The synthesis techniques reported here allow for the deposition of high-quality materials using a single tube furnace setup. This single furnace apparatus eliminates the need for multiple deposition systems, leading to reduced operating costs. Transfer has been achieved using polymer-assisted methods, and material quality has been characterized using optical and electron microscopy techniques. This work provides invaluable information for infrastructure setup and detailed procedures for material synthesis, transfer, and characterization.				
15. SUBJECT TERMS graphene, hexagonal boron nitride, bismuth telluride, synthesis, transfer, characterization				
16. SECURITY CLASSIFICATION OF:		17. LIMITATION OF ABSTRACT UU	18. NUMBER OF PAGES 24	19a. NAME OF RESPONSIBLE PERSON Mark Griep
a. REPORT Unclassified	b. ABSTRACT Unclassified			c. THIS PAGE Unclassified

Contents

List of Figures	iv
Acknowledgments	v
1. Introduction and Background	1
2. Materials and Methods	1
3. Results and Discussion	2
3.1 Copper Foil Preparation	2
3.2 Graphene Synthesis and Transfer	2
3.3 Hexagonal Boron Nitride Synthesis and Transfer	5
3.4 Bismuth Telluride Synthesis and Transfer	7
4. Summary and Conclusions	10
5. References	11
List of Symbols, Abbreviations, and Acronyms	15
Distribution List	16

List of Figures

Fig. 1	Chemical vapor deposition (CVD) furnace showing vacuum lines and temperature controller	3
Fig. 2	Growth profile for single layer graphene on copper via CVD.....	3
Fig. 3	Characterization of graphene domains and adlayers. a) Laser scanning image of graphene on copper foil. The inset shows the corresponding white light image. b) Graphene domains transferred to 285-nm SiO ₂ /Si. c) SEM image of single graphene domain with multiple adlayers formed in the center. d) Raman spectra of colored regions marked in (c).	5
Fig. 4	Growth profile for CVD synthesis of hBN	6
Fig. 5	SEM characterization of hBN on copper at different levels of magnification. a) 10 K, b) 18 K, c) 20 K, and d) 40 K. The red arrows indicate wrinkles in the film.	7
Fig. 6	Growth profile for vapor transport synthesis of Bi ₂ Te ₃	8
Fig. 7	Substrate placement and position relative to flow direction for Bi ₂ Te ₃ synthesis	8
Fig. 8	Characterization of Bi ₂ Te ₃ nanoplates. a) Optical micrograph of hexagonal and triangular-shaped plates on 285 nm of SiO ₂ /Si. The inset shows the corresponding CLSM image. b) SEM image of plates synthesized on Si. c) TEM image of hexagonal plate showing well-defined edges. d) EDS spectrum of plate shown in (c). The inset shows the corresponding Raman spectra.	9

Acknowledgments

This research was supported in part by an appointment to the Research Participation Program at the US Army Research Laboratory (ARL) administered by the Oak Ridge Institute for Science and Education through an interagency agreement between the US Department of Energy and ARL. The authors also want to acknowledge Dr Scott Walck for his invaluable guidance in transmission electron microscopy-related issues and Dr Shashi P Karna for his support.

INTENTIONALLY LEFT BLANK.

1. Introduction and Background

Two-dimensional (2-D) nanomaterials have recently attracted much attention because of their unique electronic and mechanical properties not found in their bulk counterparts.^{1–5} Graphene and hexagonal boron nitride (hBN) are 2 honeycomb lattice 2-D materials that make up the bulk of the most recent literature.^{6–12} The excellent thermal, mechanical, and electrical properties, along with their numerous synthesis routes, make graphene and hBN ideal building blocks for 2-D material infrastructure. Another 2-D material that is being studied more recently is nanoscale bismuth telluride (Bi_2Te_3). The unique surface states and the material's ability to act as a topological insulator make Bi_2Te_3 a suitable choice for coupling with graphene/hBN systems.^{13–15} Although much work has been carried out on the individual growth and optimization of graphene, hBN, and Bi_2Te_3 , a single system that is capable of synthesizing each material has yet to be realized. The ability to fabricate structures based on the integration of these materials relies on the scalability and cost to produce the individual components. Having infrastructure that is capable of producing high-quality materials that are reproducible will be a key factor in rapid, low-cost device manufacturing. The promise for the integration of these materials lies in the ability to use a single tube furnace system to synthesize each individual component.

In the present work, graphene, hBN, and Bi_2Te_3 have been synthesized and optimized using a hot-wall tube furnace system. Methods for device transfer have also been optimized using either polymer-assisted or wet chemical techniques. Various characterization techniques have also been performed to determine material quality and structure. This study will lay the framework for the development of a 2-D nanomaterial infrastructure across a broad depth of institutions, including academia, government, and industry.

2. Materials and Methods

Copper foils (25 μm , 99.8%) were purchased from Alfa Aesar and electropolished prior to growth.

Ethanol, isopropyl alcohol, urea, and phosphoric acid were purchased from Sigma-Aldrich (St. Louis, MO) and used as received. For material precursors, Bi_2Te_3 powder (733482-5G) and ammonia borane (682098-10G) were used as received.

A 1-inch split tube furnace (MTI OTF-1200X) with 1-m quartz tubes was used for material synthesis. A 3-channel mass flow controller (MTI Corp.) was used to control gas flow rates. The precursor gases were purchased from Airgas with

composition and purity as follows: H₂ (99.999%), Ar (99.999%), and CH₄ (99.999%).

The domain size and shape of the synthesized materials were characterized using an Olympus OLS3100 utilizing a confocal laser scanning microscopy (CLSM) technique. A 405-nm laser was used as the excitation source and intensity were adjusted based on sample reflectance. To increase the contrast between the graphene and copper foil, samples were thermally annealed in air at 200 °C for 10 s. Raman spectra were taken using a Horiba LabRAM ARAMAS system with an excitation wavelength of 532 nm. Scanning electron microscopy (SEM) images were taken with a Hitachi S4700 microscope. Transmission electron microscopy (TEM) was carried out using a JEOL 2100 microscope.

3. Results and Discussion

3.1 Copper Foil Preparation

Copper foils (Alfa Aesar, 25 µm, 99.8%) were cleaned and degreased using an acetone, isopropyl alcohol, and milli-Q water rinse process prior to polishing. This procedure involves sequential dipping of the foils in each solution until the surface is fully wetted. After a final rinse in milli-Q, the foils are immediately placed on the polishing unit. Reducing the copper surface roughness was carried out using a Struers Lectropol 5 automatic electropolishing unit. A mixture comprising 330 mL of deionized, distilled (DDI) water, 167 mL of orthophosphoric acid, 167 mL of ethanol, 33 mL of isopropyl alcohol, and 3.3 g of urea was used as the polishing electrolyte solution. Copper foils were prepared with an electropolished sample area of 5 cm². Electropolishing was performed across a potential of 8 V with a constant flow rate of 12 for the designated polishing time. After polishing, samples were rinsed by sequential dipping in a DDI bath followed by a final rinse with isopropyl alcohol. Samples were then dried with a soft stream of nitrogen.

3.2 Graphene Synthesis and Transfer

Graphene domains were synthesized using a low-pressure chemical vapor deposition technique. After polishing, copper samples were loaded into a 1-inch quartz tube furnace and evacuated to the base vacuum pressure of 50 mTorr. A picture of the system is shown in Fig. 1. Hydrogen was then introduced into the system, resulting in a chamber pressure of 350 mTorr. Samples were then rapidly heated to 1,060 °C by moving the foils within the heated zone of the furnace and annealed for 30 min in a hydrogen environment. For full coverage graphene, methane was then introduced into the system at a pressure of 150 mTorr for 20 min.

Growth can be stopped from 1 to 5 min for nucleation. A schematic of the growth profile is shown in Fig. 2.



Fig. 1 Chemical vapor deposition (CVD) furnace showing vacuum lines and temperature controller

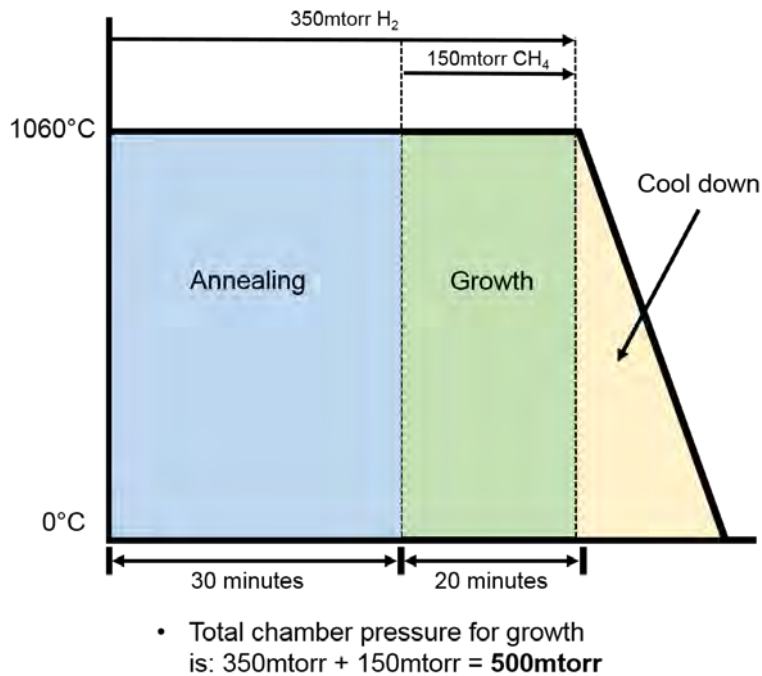


Fig. 2 Growth profile for single layer graphene on copper via CVD

After growth, methane was shut off and samples were rapidly cooled ($100\text{ }^{\circ}\text{C/min}$) to room temperature in a hydrogen atmosphere. A polymer-assisted method was used for graphene transfer.¹⁶⁻²⁰ Briefly, 1 wt % poly(bisphenol A) carbonate (PC)

in chloroform was spin coated (5,000 rpm for 1 min) on a graphene/copper foil sample. Samples were then floated on top of a 0.1-M solution of ammonium persulfate for approximately 2 h until no copper was visible. After which, samples were rinsed in 3 successive baths of DDI water. Samples were then transferred to silicon dioxide/silicon (SiO_2/Si) (285 nm thermal oxide) and allowed to dry in air. Polymer was then removed by rinsing the sample with chloroform and blow drying with nitrogen. To fabricated multilayer graphene samples, a stacking technique can be used. The procedure is similar to the normal transfer process. After going through the final rinsing procedure, a polymer/graphene stack is floating on top of the DDI water surface. Instead of removing the stack with the target substrate, a graphene/copper foil substrate (graphene side up) can be used to remove the layer. This will result in the following stacking order (top to bottom): polymer/graphene layer 1/graphene layer 2/copper. The substrate should then be allowed to dry in air until the top polymer/graphene layer is well adhered to the bottom substrate. This is evidenced when there are no wrinkles in the polymer film. After drying, a second layer of polymer should be spin coated on top of the substrate. This will provide extra support and ensure that all graphene is transferred. The copper foil can then be etched away and the substrate rinsed using the normal procedure. This process can be repeated for additional layers of graphene.

Graphene quality, domain size, and structure characterization were carried out using Raman spectroscopy, and optical and electron microscopy. Figure 3 outlines the characterization for graphene domains. For rapid optical characterization of the domains directly on copper, the foils can be annealed in air at 160 °C for 5 min. This thermal treatment results in the growth of an oxide layer where the copper is not protected by the graphene. The resulting contrast between the graphene-protected copper and the oxidized copper makes it easy to distinguish the size and shape of the domains using white light.²¹

CLSM is a technique that uses stacked 2-D images to create a 3-D profile. Using the raw reflected light intensity,²² one can image the formation of graphene adlayers, as shown in Fig. 3a. This technique does not achieve the resolution afforded with SEM; however, the high-throughput nature of the characterization (~5 min) makes it a valuable method for system optimization. Graphene adlayers can also be readily imaged in white light by transferring the domains onto 285-nm SiO_2/Si substrate. Graphene domains transferred onto SiO_2/Si are shown in Fig 3b. The unique optical interference between the graphene and oxide layer make the domains easily distinguishable against the underlying substrate.^{23–27} For higher-resolution imaging, SEM can be used. Figure 3c shows a single domain and the darker adlayer regions. The surface sensitive secondary electrons in conjunction with the upper-level detector allow for high-resolution images of the domains and

their central adlayers. The atomic level spacing between the layers makes surface sensitive SEM characterization the ideal method for determining the adlayer size and number of layers. Raman spectroscopy is another technique used for determining the quality of the graphene as well as the number of layers. The spectrum for single- and up to 4-layer graphene are shown in Fig 3d. Graphene quality can be quantified by determining the intensity of the so-called defect peak, D ($1,350\text{ cm}^{-1}$), relative to the G peak ($1,597\text{ cm}^{-1}$).²⁸ The graphene in our experiments showed very little signal from the D peak, indicating nearly defect-free domains. Determining the number of layers can also be determined by examining the ratio of the 2-D peak ($2,700\text{ cm}^{-1}$) to the G peak.²⁹ For a single layer, this ratio is between 2 and 4, while bilayer graphene has a 1:1 ratio. Additional layers of graphene decrease the ratio even further as the material transitions to a more bulk state.³⁰

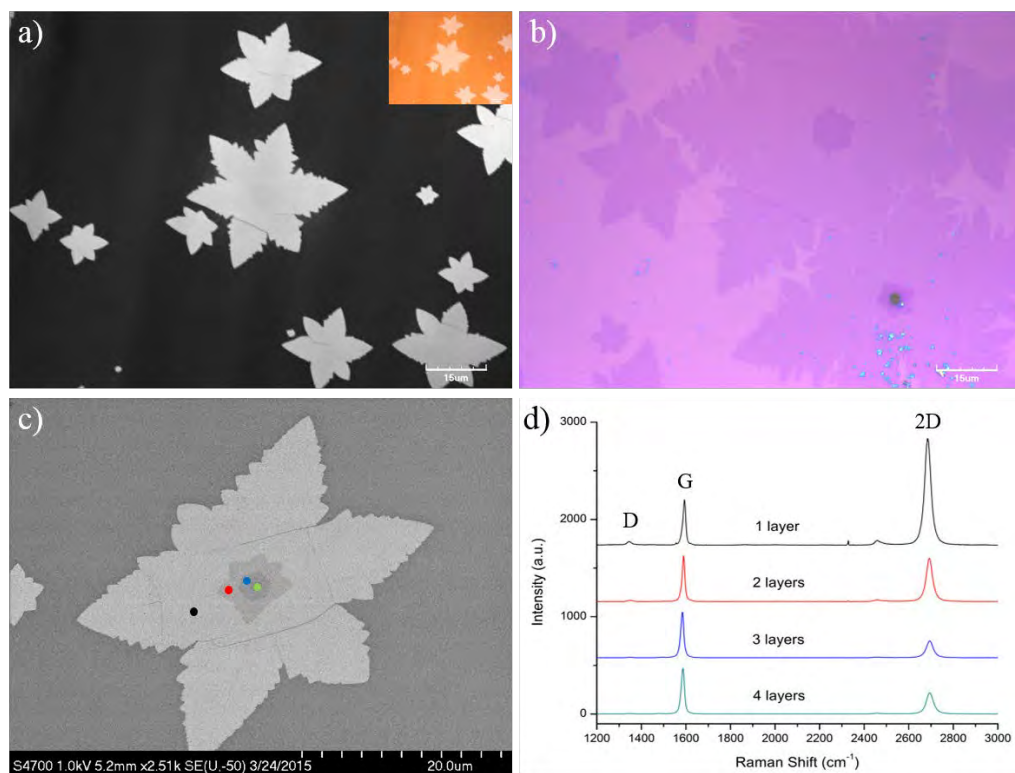


Fig. 3 Characterization of graphene domains and adlayers. a) Laser scanning image of graphene on copper foil. The inset shows the corresponding white light image. b) Graphene domains transferred to 285-nm SiO₂/Si. c) SEM image of single graphene domain with multiple adlayers formed in the center. d) Raman spectra of colored regions marked in (c).

3.3 Hexagonal Boron Nitride Synthesis and Transfer

Hexagonal boron nitride synthesis was carried out using a low-pressure CVD technique. Polished copper foils were loaded into a 1-inch quartz furnace and

evacuated to the base vacuum pressure of 50 mTorr. The precursor ammonia borane powder (5 mg) was placed in a quartz boat and positioned 30 cm away from the center of the hot zone of the furnace. Hydrogen was then introduced into the system, resulting in an increase of chamber pressure to 450 mTorr. Copper foils were then annealed for 30 min in a hydrogen atmosphere by moving the foils into the heated zone of the furnace. The ammonia borane was then heated to 100 °C using a heating belt, and argon was used as the carrier gas with a chamber partial pressure of 1 Torr. Full coverage films can be attained using a growth time of 5 min. For hBN nucleation, growth time can be reduced to 1 min. After growth, the heating belt was shut off along with the argon. The foils were rapidly cooled (100 °C/min) in a hydrogen environment by sliding the furnace away from the substrate. Air was then used to purge and bring the system back to atmospheric pressure. The growth profile is outlined in Fig. 4.

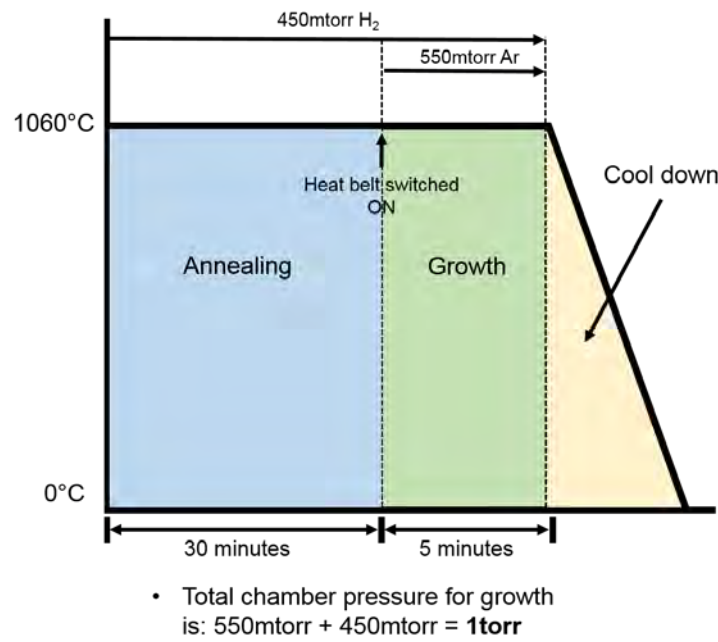


Fig. 4 Growth profile for CVD synthesis of hBN

Transferring hBN is accomplished using the same techniques as for graphene transfer, which are outlined in detail in Section 3.2.

Characterizing hBN growth is achieved most readily using SEM. Figure 5 shows multilayer hBN domains synthesized on copper foils at multiple magnifications. The triangular shape of the domains is a result of the nitrogen terminated edges.^{31,32} The growth of full coverage films is evidenced through the formation of wrinkles throughout the surface. As a result of the high-temperature growth process, wrinkle formation is seen in the hBN, owing to the difference in coefficient of thermal expansion between the copper foil substrate and hBN film.³³

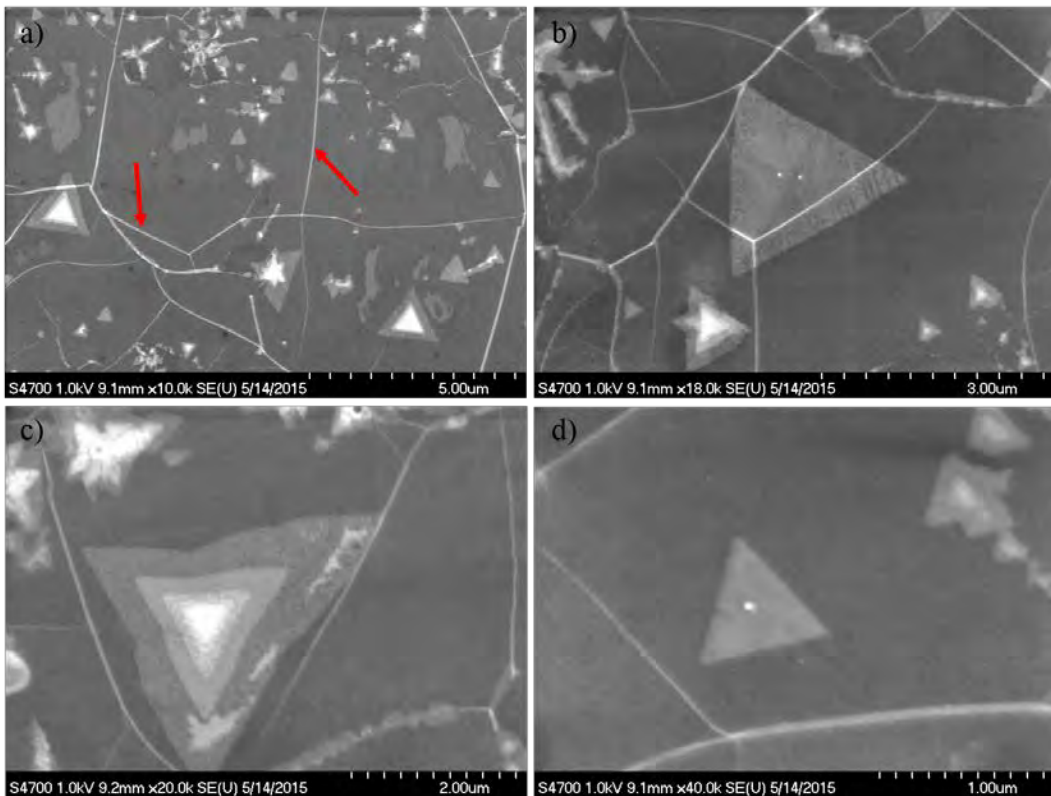


Fig. 5 SEM characterization of hBN on copper at different levels of magnification. a) 10 K, b) 18 K, c) 20 K, and d) 40 K. The red arrows indicate wrinkles in the film.

Since hBN has a different electronic band structure compared to graphene, the interference between hBN and SiO₂/Si is much less pronounced.^{34,35} This makes it difficult to optically identify the individual domains.

3.4 Bismuth Telluride Synthesis and Transfer

A physical vapor deposition (PVD) process was used to synthesize Bi₂Te₃ nanoplates. The mechanism of formation for nanoplates is governed via vapor-solid processes.³⁶ The precursor powder is heated near the melting point, causing material vaporization. The carrier gas then transports the heated vapor along the direction of flow. The vaporized material is then deposited outside the heating zone on the tube and target substrates. In this work, piranha-etched SiO₂/Si and Si wafers were used as growth substrates. A typical piranha cleaning involves a 3:1 mixture of sulfuric acid to hydrogen peroxide. This mixture is highly dangerous and should be handled using appropriate personal protection equipment.

To begin, the wafers should be precleaned in an acetone bath under sonication for 30 min. This will remove any residue left from the backside adhesive along with loose contaminants. Sulfuric acid should then be added to a separate container,

followed by slowly pouring hydrogen peroxide into the solution. The mixture will get hot (120°C) and may bubble. After adding the hydrogen peroxide, immediately add the wafers. Allow 10 min for cleaning, then carefully remove substrates from the solution, rinse with DDI, and dry with nitrogen. The substrates are now ready for growth.

Growth is carried out in a 1-inch tube furnace. The growth profile is outlined in Fig. 6. Prior to adding substrates to the furnace, 0.2 mg of Bi_2Te_3 precursor was weighed and placed into a ceramic boat. The substrates were then placed inside the tube, 10 cm away from the center of the heat zone. The precursor was then placed in the middle of the heat zone. The optimum furnace setup for nanoplate growth is shown in Fig. 7.

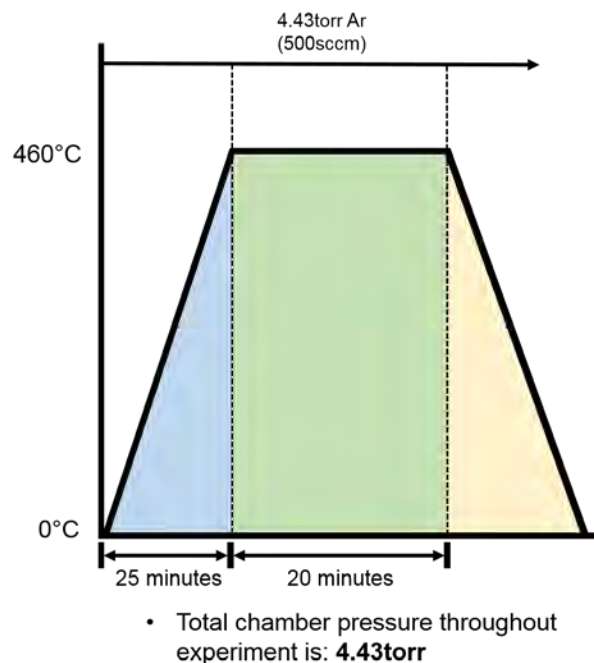


Fig. 6 Growth profile for vapor transport synthesis of Bi_2Te_3

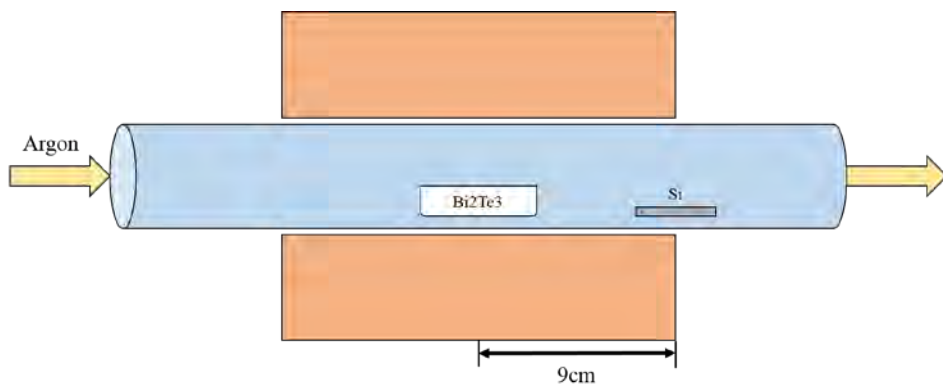


Fig. 7 Substrate placement and position relative to flow direction for Bi_2Te_3 synthesis

The tube was pumped down to a vacuum pressure of 50 mTorr; 500 standard cubic centimeters per minute of argon was then introduced into the system, resulting in a chamber pressure of 4.43 Torr. This condition was used throughout the heating, growth, and cool-down portions of the synthesis. The chamber was then heated to 460 °C in 25 min. The system was held at that temperature for 20 min for nanoplate formation. The system was then allowed to cool down naturally to room temperature. Figure 8 shows the synthesized Bi₂Te₃ nanoplates.

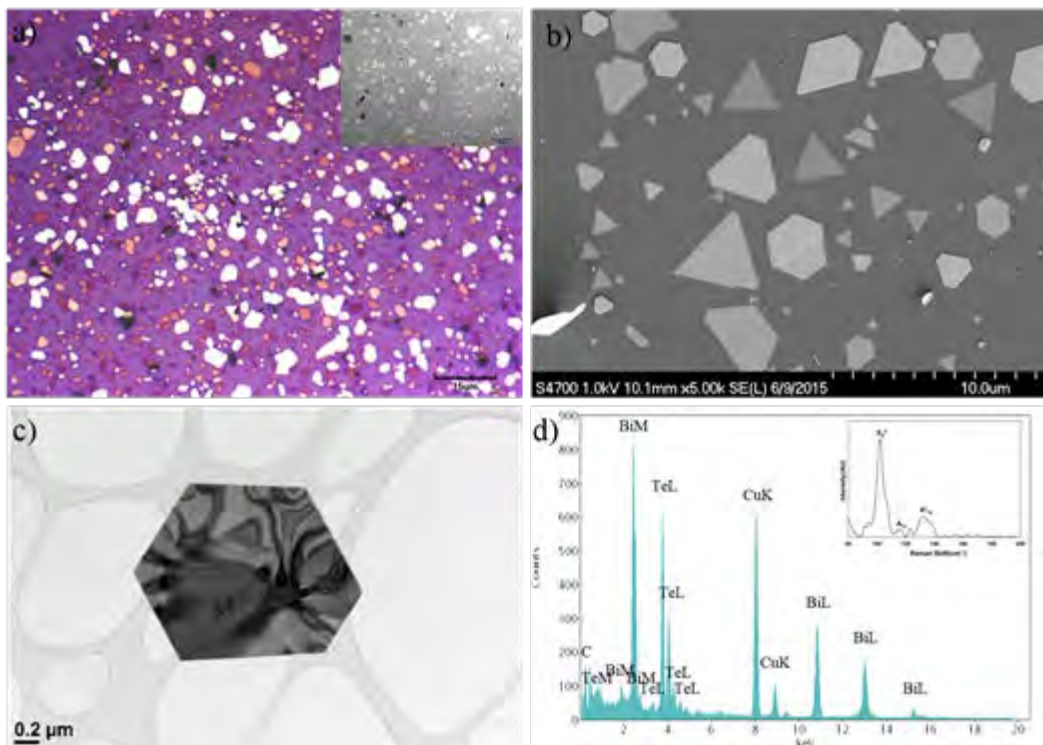


Fig. 8 Characterization of Bi₂Te₃ nanoplates. a) Optical micrograph of hexagonal and triangular-shaped plates on 285 nm of SiO₂/Si. The inset shows the corresponding CLSM image. b) SEM image of plates synthesized on Si. c) TEM image of hexagonal plate showing well-defined edges. d) EDS spectrum of plate shown in (c). The inset shows the corresponding Raman spectra.

Most of the characterization techniques can be carried out using the Si or SiO₂/Si growth substrates. However, for TEM and additional experiments, the nanoplates must be transferred to appropriate substrates. This can be accomplished using a cellulose acetate transfer film method. A detailed procedure for transfer is published elsewhere.³⁷ In brief, several drops of acetone are placed on the sample surface. Before the acetone is allowed to evaporate, an acetate film is placed on the surface carefully from one end to the other. Surface tension allows the film to be pulled to the surface, reducing the formation of bubbles. After drying for approximately 30 min, the acetate film is carefully removed from the surface. This acetate film contains the synthesized materials and does not damage the sample.

This film can then be placed, sample side facing down, on the target substrate. After placing on the target substrate, acetone is dropped on the film and allowed to absorb into the acetate. The sample can then be rinsed in successive baths of acetone to remove the transfer film.

4. Summary and Conclusions

In the current study, graphene, hBN, and Bi_2Te_3 have been synthesized using CVD and PVD techniques. Transfer of materials was accomplished using polymer and acetate-assisted methods. Optical, spectral, and electron microscopy techniques were then used for characterization. This work provides detailed procedures for the development of 2-D nanomaterial infrastructure using a single tube furnace system. Additional experiments can be carried out using this methodology to create tailored materials for applications in energy harvesting and storage, water filtration, and electronics.

5. References

1. Mas-Balleste R, Gomez-Navarro C, Gomez-Herrero J, Zamora F. 2-D materials: to graphene and beyond. *Nanoscale*. 2011;3(1):20–30.
2. Butler SZ, Hollen SM, Cao L, Cui Y, Gupta JA, Gutierrez HR, Goldberger JE. Progress, challenges, and opportunities in two-dimensional materials beyond graphene. *ACS Nano*. 2013;7(4):2898–2926.
3. Xu M, Liang T, Shi M, Chen H. Graphene-like two-dimensional materials. *Chemical Reviews*. 2013;113(5):3766–3798.
4. Koski KJ, Cui Y. The new skinny in two-dimensional nanomaterials. *ACS Nano*. 2013;7(5):3739–3743.
5. Zhuang X, Mai Y, Wu D, Zhang F, Feng X. Two-dimensional soft nanomaterials: a fascinating world of materials. *Advanced Materials*. 2015;27(3):403–427.
6. Allen MJ, Tung VC, Kaner RB. Honeycomb carbon: a review of graphene. *Chemical Reviews*. 2009;110(1):132–145.
7. Choi W, Lahiri I, Seelaboyina R, Kang YS. Synthesis of graphene and its applications: a review. *Critical Reviews in Solid State and Materials Sciences*. 2010;35(1):52–71.
8. Mattevi C, Kim H, Chhowalla M. A review of chemical vapour deposition of graphene on copper. *Journal of Materials Chemistry*. 2011;21(10):3324–3334.
9. Geim AK, Novoselov KS. The rise of graphene. *Nature Materials*. 2007;6(3):183–191.
10. Shi Y, Hamsen C, Jia X, Kim KK, Reina A, Hofmann M, Kong J. Synthesis of few-layer hexagonal boron nitride thin film by chemical vapor deposition. *Nano Letters*. 2010;10(10):4134–4139.
11. Song L, Ci L, Lu H, Sorokin PB, Jin C, Ni J, Ajayan PM. Large scale growth and characterization of atomic hexagonal boron nitride layers. *Nano Letters*. 2010;10(8):3209–3215.
12. Kim KK, Hsu A, Jia X, Kim SM, Shi Y, Hofmann M, Kong J. Synthesis of monolayer hexagonal boron nitride on Cu foil using chemical vapor deposition. *Nano Letters*. 2011;12(1):161–166.

13. Kong D, Dang W, Cha JJ, Li H, Meister S, Peng H, Cui Y. Few-layer nanoplates of Bi_2Se_3 and Bi_2Te_3 with highly tunable chemical potential. *Nano Letters*. 2010;10(6):2245–2250.
14. Lu W, Ding Y, Chen Y, Wang ZL, Fang J. Bismuth telluride hexagonal nanoplatelets and their two-step epitaxial growth. *Journal of the American Chemical Society*. 2005;127(28):10112–10116.
15. Teweldebrhan D, Goyal V, Balandin AA. Exfoliation and characterization of bismuth telluride atomic quintuples and quasi-two-dimensional crystals. *Nano Letters*. 2010;10(4):1209–1218.
16. Lin YC, Jin C, Lee JC, Jen SF, Suenaga K, Chiu PW. Clean transfer of graphene for isolation and suspension. *ACS Nano*. 2011;5(3):2362–2368.
17. Lee Y, Bae S, Jang H, Jang S, Zhu SE, Sim SH, Ahn JH. Wafer-scale synthesis and transfer of graphene films. *Nano Letters*. 2010;10(2):490–493.
18. Liang X, Sperling BA, Calizo I, Cheng G, Hacker CA, Zhang Q, Richter CA. Toward clean and crackless transfer of graphene. *ACS Nano*. 2011;5(11):9144–9153.
19. Kang J, Shin D, Bae S, Hong BH. Graphene transfer: key for applications. *Nanoscale*. 2012;4(18):5527–5537.
20. Li X, Zhu Y, Cai W, Borysiak M, Han B, Chen D, Ruoff RS. Transfer of large-area graphene films for high-performance transparent conductive electrodes. *Nano Letters*. 2009;9(12):4359–4363.
21. Jia C, Jiang J, Gan L, Guo X. Direct optical characterization of graphene growth and domains on growth substrates. *Scientific Reports*. 2012;2:1038–1044.
22. Tumlin TM, Griep MH, Sandoz-Rosado E, Karna SP. Modeling graphene contrast on copper surfaces using optical microscopy. Aberdeen Proving Ground (MD): Army Research Laboratory (US); 2014. Report No.: ARL-TR-7134.
23. Blake P, Hill EW, Neto AC, Novoselov KS, Jiang D, Yang R, Geim AK. Making graphene visible. *Applied Physics Letters*. 2007;91(6):063124.
24. Abergel DSL, Russell A, Fal'ko VI. Visibility of graphene flakes on a dielectric substrate. *Applied Physics Letters*. 2007;91:063125. arXiv preprint arXiv:0705.0091.

25. Roddarro S, Pingue P, Piazza V, Pellegrini V, Beltram F. The optical visibility of graphene: interference colors of ultrathin graphite on SiO₂. *Nano Letters*. 2007;7(9):2707–2710.
26. Jung I, Pelton M, Piner R, Dikin DA, Stankovich S, Watcharotone S, Ruoff RS. Simple approach for high-contrast optical imaging and characterization of graphene-based sheets. *Nano Letters*. 2007;7(12):3569–3575.
27. Teo G, Wang H, Wu Y, Guo Z, Zhang J, Ni Z, Shen Z. Visibility study of graphene multilayer structures. *Journal of Applied Physics*. 2008;103(12):124302.
28. Malard LM, Pimenta MA, Dresselhaus G, Dresselhaus MS. Raman spectroscopy in graphene. *Physics Reports*. 2009;473(5):51–87.
29. Ferrari AC, Meyer JC, Scardaci V, Casiraghi C, Lazzeri M, Mauri F, Geim AK. Raman spectrum of graphene and graphene layers. *Physical Review Letters*. 2006;97(18):187401.
30. Ni Z, Wang Y, Yu T, Shen Z. Raman spectroscopy and imaging of graphene. *Nano Research*. 2008;1(4):273–291.
31. Jin C, Lin F, Suenaga K, Iijima S. Fabrication of a freestanding boron nitride single layer and its defect assignments. *Physical Review Letters*. 2009;102(19):195505.
32. Alem N, Erni R, Kisielowski C, Rossell MD, Gannett W, Zettl A. Atomically thin hexagonal boron nitride probed by ultrahigh-resolution transmission electron microscopy. *Physical Review B*. 2009;80(15):155425.
33. Kim KK, Hsu A, Jia X, Kim SM, Shi Y, Hofmann M, Kong J. Synthesis of monolayer hexagonal boron nitride on Cu foil using chemical vapor deposition. *Nano Letters*. 2011;12(1):161–166.
34. Giovannetti G, Khomyakov PA, Brocks G, Kelly PJ, van den Brink J. Substrate-induced band gap in graphene on hexagonal boron nitride: ab initio density functional calculations. *Physical Review B*. 2007;76(7):073103.
35. Watanabe K, Taniguchi T, Kanda H. Direct-bandgap properties and evidence for ultraviolet lasing of hexagonal boron nitride single crystal. *Nature Materials*. 2004;3(6):404–409.
36. Wagner RS, Ellis WC. Vapor-liquid-solid mechanism of single crystal growth. *Applied Physics Letters*. 1964;4(5):89–90.

37. Replication Materials for Microscopy. PELCO® technical notes, cellulose acetate replicating film; Redding (CA): Ted Pella, Inc. n.d. [accessed 2015 Aug 03]. http://www.tedpella.com/replicat_html/44840.htm

List of Symbols, Abbreviations, and Acronyms

2-D	2-dimensional
Ar	argon
Bi ₂ Te ₃	bismuth telluride
DDI	deionized, distilled
CLSM	confocal laser scanning microscopy
CVD	chemical vapor deposition
hBN	hexagonal boron nitride
H ₂	hydrogen
PC	poly (bisphenol A) carbonate
PVD	physical vapor deposition
SEM	scanning electron microscopy
Si	silicon
SiO ₂	silicon dioxide
TEM	transmission electron microscopy

1 DEFENSE TECHNICAL
(PDF) INFORMATION CTR
DTIC OCA

2 DIRECTOR
(PDF) US ARMY RESEARCH LAB
RDRL CIO LL
IMAL HRA MAIL & RECORDS
MGMT

1 GOVT PRINTG OFC
(PDF) A MALHOTRA

1 DIR USARL
(PDF) RDRL WMM A
M GRIEP